The Journal of Immunology

Mechanism Regulating Reactive Oxygen Species in Tumor-Induced Myeloid-Derived Suppressor Cells

Cesar A. Corzo, Matthew J. Cotter, Pingyan Cheng, Fendong Cheng, Sergei Kusmartsev, Eduardo Sotomayor, Tapan Padhya, Thomas V. McCaffrey, Judith C. McCaffrey and Dmitry I. Gabrilovich

J Immunol 2009; 182:5693-5701; ;
doi: 10.4049/jimmunol.0900092
http://www.jimmunol.org/content/182/9/5693

The Journal of Immunology is published twice each month by
The American Association of Immunologists, Inc.,
1451 Rockville Pike, Suite 650, Rockville, MD 20852

Print ISSN: 0022-1767 Online ISSN: 1550-6606.

Mechanism Regulating Reactive Oxygen Species in Tumor-Induced Myeloid-Derived Suppressor Cells[1]

Cesar A. Corzo,* Matthew J. Cotter,* Pingyan Cheng,* Fendong Cheng,* Sergei Kusmartsev,[2]* Eduardo Sotomayor,*‡ Tapan Padhya,*† Thomas V. McCaffrey,*† Judith C. McCaffrey,*† and Dmitry I. Gabrilovich[3]*†

Myeloid-derived suppressor cells (MDSC) are a major component of the immune suppressive network described in cancer and many other pathological conditions. Recent studies have demonstrated that one of the major mechanisms of MDSC-induced immune suppression is mediated by reactive oxygen species (ROS). However, the mechanism of this phenomenon remained unknown. In this study, we observed a substantial up-regulation of ROS by MDSC in all of seven different tumor models and in patients with head and neck cancer. The increased ROS production by MDSC is mediated by up-regulated activity of NADPH oxidase (NOX2). MDSC from tumor-bearing mice had significantly higher expression of NOX2 subunits, primarily p47^{phox} and gp91^{phox}, compared with immature myeloid cells from tumor-free mice. Expression of NOX2 subunits in MDSC was controlled by the STAT3 transcription factor. In the absence of NOX2 activity, MDSC lost the ability to suppress T cell responses and quickly differentiated into mature macrophages and dendritic cells. These findings expand our fundamental understanding of the biology of MDSC and may also open new opportunities for therapeutic regulation of these cells in cancer. ***The Journal of Immunology,*** **2009, 182: 5693–5701.**

The inability of T cells to mount an effective antitumor response, even following vaccination, is an immunological hallmark of cancer and represents a critical problem for the development of effective immunotherapeutic strategies. Myeloid-derived suppressor cells (MDSC)[4] are one of the major components of the immune suppressive network responsible for T cell nonresponsiveness in cancer. MDSC are a large group of myeloid cells consisting of immature macrophages, granulocytes, and dendritic cells as well as myeloid cells at earlier stages of differentiation (reviewed in Ref. 1–3). In mice, MDSC express both the myeloid lineage differentiation Ag Gr-1 (Ly6G and Ly6C) and α_M integrin CD11b, and during tumor development this population undergoes dramatic expansion. In many tumor models, the proportion of MDSC represents >20% of all splenocytes and MDSC are easily detectable in tumors and lymph nodes (1, 2, 4). Similar expansion, albeit to a lesser degree, is observed in patients with cancer. In humans, MDSC are generally defined as cells that express CD11b and the common myeloid marker CD33, but lack the expression of markers of mature myeloid and lymphoid cells and the MHC class II molecule HLA-DR (5–7). In the presence of appropriate cytokines in vitro and after adoptive transfer in vivo, MDSC can differentiate into mature myeloid cells (8). This differentiation is blocked, however, in the presence of tumor-cell-conditioned medium or in tumor-bearing hosts (3).

Evidence suggests that in peripheral lymphoid organs, MDSCs may mediate Ag-specific T cell tolerance by taking up soluble Ags, including tumor-associated Ags, processing, and presenting them to T cells (9–11). In recent years, reactive oxygen species (ROS) have been implicated in MDSC-mediated T cell suppression in peripheral lymphoid organs (10, 12–16), and it has been suggested that ROS could be responsible for the Ag-specific nature of MDSC-mediated suppression of T cell responses. Increased level of ROS was found to be also involved in inhibition of MDSC differentiation to mature myeloid cells (8, 14). However, it remained unclear whether up-regulation of ROS is a general characteristic of MDSC from different tumor models and whether it can be observed in patients' MDSC. The mechanism responsible for increased ROS production by MDSC is also unknown. In this study, we report that increased ROS levels in MDSC and the ROS-mediated suppressive function of these cells is caused by up-regulation of several subunits of NADPH oxidase and that this up-regulation is controlled by the STAT3 transcription factor.

Materials and Methods

Mice and tumor models

BALB/c and C57BL/6 mice (6–8 wk of age) were obtained from the National Cancer Institute. Mice were kept in pathogen-free conditions and handled in accordance with the requirements of the Guideline for Animal Experiments. OT-1 TCR-transgenic mice (C57BL/6-Tg(TCRaTCRb)1100mjb), gp91$^{phox-/-}$ (B6.129S6-Cybbtm1Din) were purchased from The Jackson Laboratory. STAT3$^{-/-}$ mice (LysMcre/Stat3$^{flox/-}$) were generated by Dr. S. Akira (Osaka University, Osaka,

*H. Lee Moffitt Cancer Center and Research Institute and †Departments of Otolaryngology and ‡Oncologic Sciences University of South Florida, Tampa, FL, 33612

Received for publication January 12, 2009. Accepted for publication February 23, 2009.

The costs of publication of this article were defrayed in part by the payment of page charges. This article must therefore be hereby marked *advertisement* in accordance with 18 U.S.C. Section 1734 solely to indicate this fact.

[1] This work was supported by National Institutes of Health Grant 1RO1 CA 84488 (to D.I.G.) and F31 CA 123708-02 fellowship (to C.A.C.). This work has been supported in part by the Analytic Microscopy and Flow Cytometry Core Facility at the H. Lee Moffitt Cancer Center.

[2] Current address: Department of Urology, University of Florida, Gainesville, FL 32601.

[3] Address correspondence and reprint requests to Dmitry Gabrilovich, H. Lee Moffitt Cancer Center, MRC 2067, 12902 Magnolia Drive, Tampa, FL 33612. E-mail address: dmitry.gabrilovich@moffitt.org

[4] Abbreviations used in this paper: MDSC, Myeloid-derived suppressor cell; ROS, reactive oxygen species; qRT-PCR, quantative real-time PCR; ChIP, chromatin immunoprecipitation; ES cell, embryonic stem cell; IMC, immature myeloid cell; NOX2, NADPH oxidase; WT, wild type; TCCM, tumor-cell-conditioned medium; KO, knock out; LIF, leukemia inhibitory factor; CGD, chronic granulomatous disease; DCFDA, dichlorodihydrofluorescein diacetate.

www.jimmunol.org/cgi/doi/10.4049/jimmunol.0900092

Japan). LysMcre mice were crossed with $Stat3^{flox/+}$ mice to generate LysMcre/$Stat3^{flox/-}$ mice (experimental group). LysMcre/$Stat3^{flox/+}$ mice from these crosses were used as littermate controls.

The following s.c. tumor models were used in this study. In BALB/c mice: DA3 mammary carcinoma (provided by D. Lopez, University of Miami, Miami, FL), CT26 colon carcinoma (American Type Culture Collection (ATCC), Manassas, VA), and MethA sarcoma (provided by L. J. Old, Ludwig Institute for Cancer Research, New York, NY). In C57BL/6 mice: EL4 thymoma (ATCC), Lewis lung carcinoma, MC38 colon carcinoma (provided by I. Turkova, University of Pittsburgh, Pittsburgh, PA), and C3 sarcoma (provided by W. Kast, University of Southern California, Los Angeles, CA). The number of tumor cells injected s.c. was different for each model and was selected based on the ability to form a tumor with 1.5 cm diameter within 2–3 wk of injection.

OVA-derived (H-$2K^b$, SIINFEKL) and control (H-$2K^b$ RAHYNIVTF) peptides were obtained from American Peptide Company.

Patients

Five patients (47–78 years old) with resectable T3 or T4 and N2b stage of head and neck cancer were enrolled in the study after signing Institutional Review Board approved consent. Patients did not receive radiation or chemotherapy for at least 3 mo before sample collection. Peripheral blood was collected for direct comparison to blood from five healthy donor control subjects. All cell samples were analyzed within 3 h following collection. Cells were loaded with dichlorodihydrofluorescein diacetate (DCFDA) and stimulated with PMA where appropriate. To identify live MDSC, mononuclear cells were labeled with a mixture of allophycocyanin-conjugated anti-CD11b, PerCP-Cy5.5-conjugated anti-CD14 and PE-Cy7-conjugated anti-CD33 Abs (BD Pharmingen). The phenotype of the cells was evaluated by multicolor flow cytometry using a LSRII flow cytometer (BD Biosciences). At least 100,000 live cells (4′,6-diamidino-2-phenylindole negative) were collected to obtain reliable data. Analysis of the samples was conducted essentially as described elsewhere (17).

Isolation of mouse cells

To collect MDSC, single cell suspensions were prepared from spleens, and red cells were removed using ammonium chloride lysis buffer. MDSC were isolated by cell sorting on a FACSAria cell sorter using staining with allophycocyanin-conjugated anti-Gr-1 and PE-conjugated anti-CD11b Abs (BD Pharmingen). In some experiments, MDSC were isolated using MiniMACS magnetic beads conjugated with streptavidin (Miltenyi Biotec) and biotinylated anti-Gr-1 Ab (BD Pharmingen).

To isolate peritoneal macrophages, mice were injected i.p. with 1 ml thiglycollate (Difco). Three days later, peritoneal cells were obtained by peritoneal lavage. Peritoneal macrophages were harvested using magnetic beads and biotinylated anti-CD11b Ab (BD Pharmingen).

ROS detection

Oxidation-sensitive dye DCFDA (Molecular Probes/Invitrogen), was used to measure ROS production by MDSC. Cells were incubated at 37°C in RPMI 1640 in the presence of 2.5 μM DCFDA for 30 min. For induced activation, cells were simultaneously cultured, along with DCFDA, with 30 ng/ml PMA (Sigma-Aldrich) and in some experiments with 2 μM ionomycin or 1 μg/ml LPS (Sigma-Aldrich). Cells were then labeled with APC-conjugated anti-Gr-1 and PE-conjugated anti-CD11b Abs on ice. Analysis was then conducted by flow cytometry as described above.

Production of H_2O_2 was quantified using Amplex Red Hydrogen Peroxide/Peroxidase Assay Kit (Invitrogen) as recommended by manufacturer. In brief, 25×10^3 cells were resuspended in HBSS (Sigma-Aldrich). After addition of PMA (30 ng/ml), the absorbance at 560 nm was measured using a microplate plate reader (Bio-Rad) at 37°C. Absorbance results were normalized to a standard curve generated by serial dilutions of 20 mM H_2O_2.

Quantative real-time PCR (qRT-PCR)

RNA was extracted with TRIzol (Invitrogen); cDNA was synthesized and used for the evaluation of gene expression as described previously (14). PCR was performed with 25 μl cDNA, TaqMan Universal PCR Master Mix (Applied Biosystems), and target gene assay mix containing sequence-specific primers and 6-carboxyfluorescein dye-labeled TaqMan minor groove binder probe (Applied Biosystems). Amplification with an 18S endogenous control assay mix was used for controls. PCR was conducted in triplicate for each sample. Data quantitation was performed using the relative standard curve method. Expression levels of the genes were normalized by 18S mRNA.

Western blotting

Cells were lysed with radioimmunoprecipitation assay buffer in the presence of protease and phosphatase inhibitors. Isolation of membrane and cytoplasmic compartments was achieved using Qproteome Cell Compartment Kit (Qiagen) according to the manufacturer's instructions. Protein lysates were subjected to 8% SDS-PAGE and transferred to PVDF membranes. Membranes were probed with appropriate specific Abs overnight at 4°C. Membranes were washed and incubated for 2 h at room temperature with secondary Ab conjugated with peroxidase. Results were visualized by chemiluminescence detection using a commercial kit (PerkinElmer). To confirm equal loading, membranes were stripped and reprobed with Ab against β-actin (Santa Cruz Biotechonology). Anti-STAT3, phospho-STAT3 Abs were obtained from Cell Signaling Technology. Abs against $gp91^{phox}$ and $p47^{phox}$ were purchased from Santa Cruz Biotechnology.

Evaluation of T cell function

Proliferation. Ag-specific proliferation was measured using OT-1 mice. Splenocytes from transgenic mice, depleted of red cells, were placed in triplicates into a *U*-bottom 96-well plate (1×10^5/well). Splenocytes were cultured in the presence of cognate Ag (OVA-derived peptide SIINFEKL) for 72 h. Eighteen hours before harvesting, cells were pulsed with [3H]thymidine (1 μCi/well; PerkinElmer). [3H]Thymidine uptake was counted using a liquid scintillation counter and expressed as cpm.

IFN-γ production. We evaluated the number of IFN-γ-producing cells in response to cognate Ag by ELISPOT assay as described (10). Each well contained 1×10^5 splenocytes from OT-1 mice. The number of spots were counted in triplicates and calculated by an automatic ELISPOT counter (Cellular Technology).

EMSA

Nuclear extracts were prepared in hypertonic buffer containing 20 mM HEPES (pH 7.9), 420 mM NaCl, 1 mM EGTA, 1 mM EDTA, 20% glycerol, 1 mM DTT, and protease and phosphatase inhibitors mixture. Extracts were normalized for total protein, and 5 μg of protein was incubated with 32P-labeled probes containing: STAT1 and STAT3 sequence, 5′-AGCTTCATTTCCCAGAAATCCCTA-3′; $p47^{phox}$ sequence, 5′-AGCTTCATTTCCCAGATATCCCTA-3′; or mutant sequence, 5′-AGCTTCATTGCACTCATATCCCTA-3′. Protein-DNA complexes were resolved by nondenaturing PAGE and detected by autoradiography.

Chromatin immunoprecipitation (ChIP) assay

32D myeloid progenitor cells were cultured in 10% FBS RPMI 1640, supplemented with IL-3. Preparation of chromatin-DNA and ChIP assay were performed using a kit from Upstate Biotechnology, anti-STAT3 Ab from Cell Signaling Technology, normal rabbit IgG from Santa Cruz Biotechnology, protein A agarose/salmon sperm DNA from Upstate Biotechnology (Millipore). Sonication was performed using Branson Sonifier (model 450, VWR Scientific). After reversal of cross-linking, purified DNA was subjected to PCR with the following primers spanning the potential STAT3 binding site in the $p47^{phox}$ promoter: 5′-AGTTAAAGGCATGTGCCACCACTG-3′, and 5′-TACACCTGCGTGCAGACATCATCT-3′. Primers for β-actin: 5′-TAGGGTGTAGACTCTTTGCAGCCA-3′, and 5′-AGCGTCTGGTTCCCAATACTGTGT-3′.

Experiments with embryonic stem (ES) cells

The R1 ES cell line was purchased from ATCC. Cells were transfected with empty RcCMV-Neo vector (R1-C) or STAT3c plasmid (R1-Stat3C) (18) using lipofectamin. ES transfectants were selected in DMEM containing G418 (0.2 mg/ml), 15% ES cell certified FBS (Life Technologies), leukocyte inhibitory factor (LIF; 1000 U, Chemocon), 0.1 mM nonessential amino acid, 100 μM 2-mecaptoethenol, and 2 mM L-glutamine.

Statistics

Statistical analysis was performed using non parametric Mann-Whitney *U* test and GraphPad Prism software. In all cases *p* values were calculated using two-sided *t* test.

Results

Hyperproduction of ROS in MDSC from tumor-bearing mice and cancer patients

Previous studies that demonstrated increased levels of ROS in MDSC were performed using only a few tumor models. Therefore, we first addressed the question whether up-regulation of ROS in

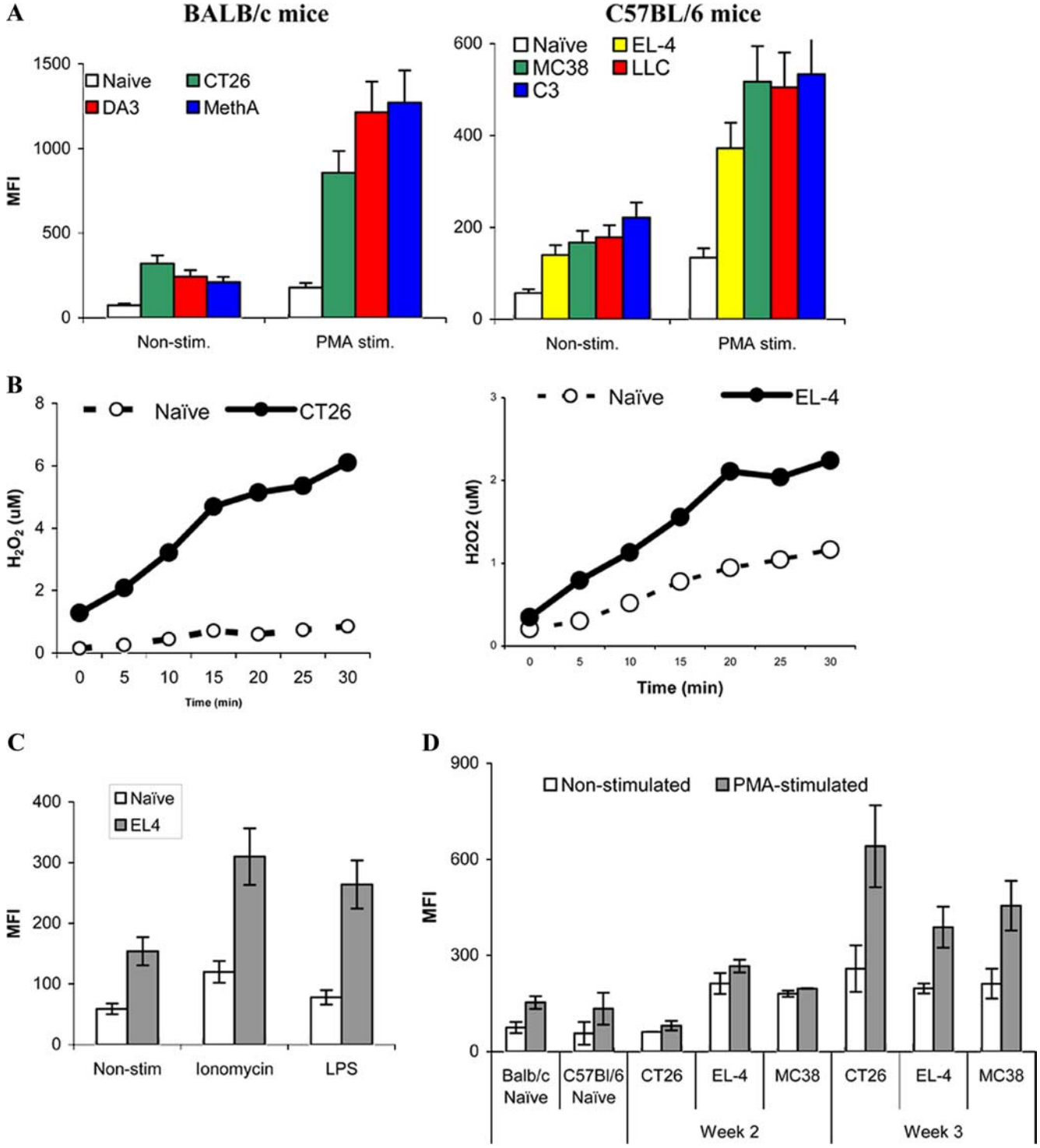

FIGURE 1. ROS level in MDSC from tumor-bearing mice. *A*, Spleens from naive tumor-free and tumor-bearing mice were collected 3 wk after tumor injection. Splenocytes were stimulated with PMA and labeled with anti-Gr-1 Ab and anti-CD11b Ab. ROS were measured in Gr-1$^+$CD11b$^+$ cells by labeling cells with the oxidation-sensitive dye DCFDA as described in *Materials and Methods*. Each group included four mice. Average and SD of the mean fluorescence intensity (MFI) are shown. *B*, H_2O_2 production by spleen MDSC from tumor-bearing mice. Gr-1$^+$ CD11b$^+$ cells were isolated from spleens of naive, CT-26, or EL-4 tumor-bearing mice and the level of H_2O_2 was measured as described in *Materials and Methods*. *C*, Splenocytes (10^6 cells) from EL-4 tumor-bearing and naive C57BL/6 mice were loaded with 2 μM DCFDA and cultured at 37°C for 30 min in RPMI 1640 in the presence of either ionomycin (2 μM) or LPS (1 μg/ml). Cells were then washed and stained with anti-Gr-1 and anti-CD11b Abs. ROS level was measured within the population of Gr-1$^+$CD11b$^+$ cells. *D*, MDSC from spleens of CT26, EL-4, and MC38 tumor-bearing mice were evaluated at different time points after tumor injection. Splenocytes were stimulated for 30 min with PMA and the production of ROS was determined in Gr-1$^+$CD11b$^+$ cells using DCFDA.

splenic MDSC was a widespread phenomenon observed in several different tumor models. Seven mouse tumor models of sarcomas, thymoma, colon, mammary, and lung carcinomas on two mouse strains (BALB/c and C57BL/6) were tested. A different number of tumor cells were injected s.c. to allow for the development of similar size tumors (1.5 cm in diameter) within 3 wk after tumor

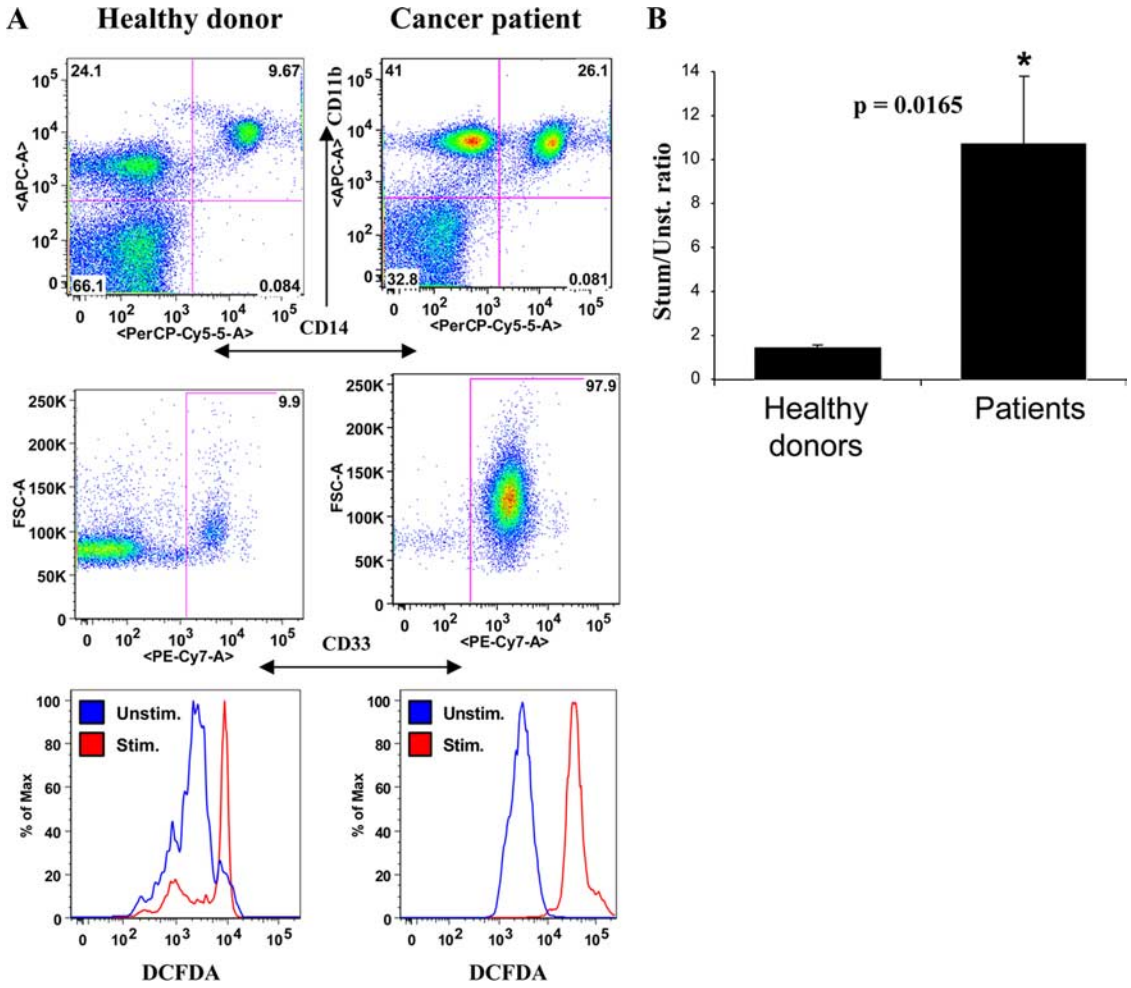

FIGURE 2. Up-regulation of ROS production in MDSC from patients with head and neck cancer. Peripheral blood MNC from healthy donors and patients with head and neck cancer were labeled with a mixture of anti-CD11b, anti-CD14 and anti-CD33-specific Abs and stained with DCFDA to detect ROS level within the population of $CD11b^+CD14^-CD33^+$ cells. *A*, The gating strategy to identify MDSC. $CD14^-CD11b^+$ cells were gated first followed by gating of $CD33^+$ cells. Histograms show representative fluorescence intensities of DCFDA in $CD14^-CD11b^+CD33^+$ MDSC from patients and donors before and after PMA stimulation. *B*, Summarized data obtained from five patients and five healthy donors. ∗, Statistically significant difference ($p < 0.05$).

inoculation. This time frame was selected as it is widely used in most studies of tumor-associated immune suppression. Splenocytes were isolated, stimulated with PMA, and labeled with anti-Gr-1 and anti-CD11b Abs to identify MDSC in tumor-bearing mice or immature myeloid cells (IMC) in naive tumor-free mice. ROS levels were measured using the oxidation-sensitive fluorescent dye DCFDA within the population of $Gr\text{-}1^+CD11b^+$ MDSC or IMC. MDSC from all tumor models without exception demonstrated a significantly ($p < 0.01$) higher level of ROS than their control counterparts (Fig. 1*A*). To verify those observations using a different experimental system, we measured the level of H_2O_2 in MDSC isolated from spleens of CT26 and EL4 tumor-bearing mice. In both models, MDSC produced substantially higher level of H_2O_2 than IMC (Fig. 1*B*). Higher level ($p < 0.05$) of ROS production by MDSC was also detected in response to other stimuli (ionomycin and LPS) indicating that this effect is not restricted to PMA (Fig. 1*C*). Furthermore, ROS levels were measured in MDSC during dynamic tumor growth. The significant increase of ROS levels in MDSC became most prominent 3 wk after tumor inoculation (Fig. 1*D*), which coincided with substantial expansion of MDSC (Ref. 12 and our unpublished observations) in these models.

To extend our studies to the clinic, we evaluated ROS levels in MDSC from patients with stage III head and neck cancer. In humans, MDSC are identifiable as lineage (CD3, CD14, CD19, CD56)-negative, HLA-DR-negative, and CD33-positive (5) or $CD11b^+$ $CD14^-$ $CD33^+$ cells (6). PBMC from healthy volunteers and patients were labeled with allophycocyanin-conjugated anti-CD11b, PerCp-Cy5.5-conjugated CD14 and PE-Cy7-conjugated anti-CD33 Abs and loaded with DCFDA. ROS levels were evaluated within the population of $CD11b^+$ $CD14^-$ $CD33^+$ cells. Patients' MDSC demonstrated an ~5-fold higher level of ROS up-regulation following PMA-stimulation compared with cells with the same phenotype from healthy volunteers ($p = 0.0165$) (Fig. 2).

Regulation of ROS production in MDSC by NAPDH oxidase

Though ROS can be produced in cells by several different mechanisms, the primary source of ROS in leukocytes is by NADPH oxidase (NOX2). The oxidase is a multicomponent enzyme consisting of two membrane proteins, $gp91^{phox}$ and $p22^{phox}$ and at least four cytosolic components: $p47^{phox}$, $p67^{phox}$, $p40^{phox}$, and a small G protein Rac (19). We measured NOX2 expression in MDSC isolated from naive tumor-free and CT-26 tumor-bearing BALB/c mice using qRT-PCR. MDSC from tumor-bearing mice had a substantially higher level of mRNA for several major NOX2 components. However, the most prominent increase was observed in the level of expression of $gp91^{phox}$ and $p47^{phox}$ (Fig. 3*A*). Increased expression of

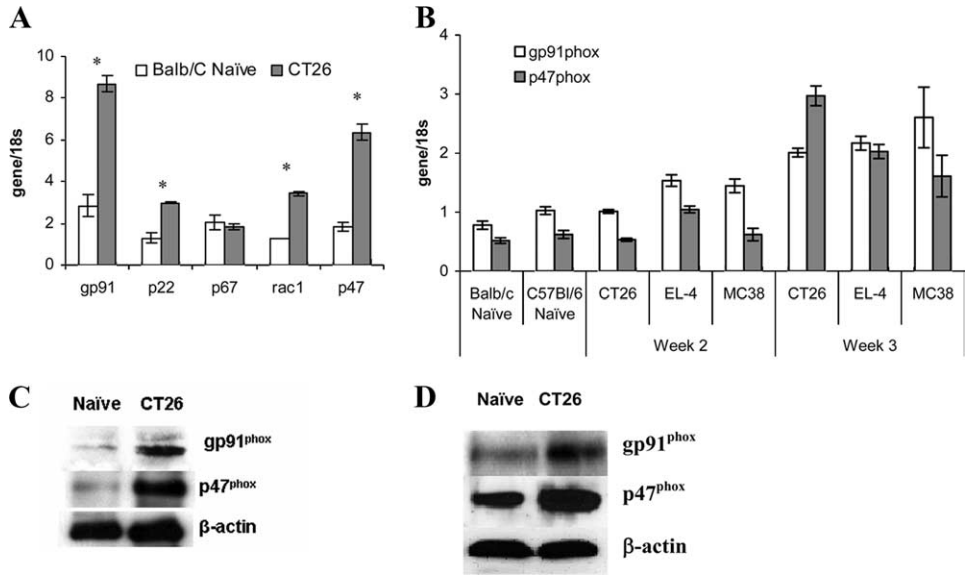

FIGURE 3. Up-regulation of NOX2 in MDSC. *A*, Gr-1$^+$ cells were isolated from spleens of naive or CT-26 tumor-bearing mice. RNA was extracted and expression of NADPH oxidase subunits was measured in triplicates by qRT-PCR. Three experiments with the same results were performed. ∗, Statistically significant difference ($p < 0.05$) between control and tumor-bearing mice. *B*, MDSC from spleens of CT26, EL-4, and MC38 tumor-bearing mice were evaluated at different time points after tumor injection. Gr-1$^+$CD11b$^+$ cells were isolated on wk 2 and 3 after injection of tumor cells and the expression of *gp91^{phox}* and *p47^{phox}* was measured by qRT-PCR. Each experiment was performed in triplicates and each group included three mice. *C* and *D*, Protein levels of gp91^{phox} and p47^{phox} were determined in total cell lysate (*C*) or membrane fractions (*D*) of isolated Gr-1$^+$CD11b$^+$ cells. Cellular fractionation was performed using a Qiagen Cell Compartment kit.

these genes was also observed in two other tested tumor models (EL-4 and MC38) (Fig. 3*B*). The most significant increase in *gp91^{phox}* and *p47^{phox}* expression was detected in mice 3 wk after tumor inoculation, which coincided with the time when the most elevated level of ROS was observed in these cells (Fig. 1*D*). The protein levels of two NOX2 components (p47^{phox} and gp91^{phox}) were analyzed further. MDSC from tumor-bearing mice had substantially higher level of p47^{phox} and gp91^{phox} proteins in whole cell lysates than IMCs from naive mice (Fig. 3*C*). Up-regulation of these proteins was also seen in the membrane fraction of MDSC from tumor-bearing mice (Fig. 3*D*). The presence of p47^{phox} in the membrane fraction of cellular proteins is indicative of NOX2 activation, because translocation of p47^{phox} to the cell membrane is required for NOX2 assembly.

Thus, increased level of ROS in MDSC was associated with up-regulation of NOX2. To investigate the potential contribution of NOX2 to the hyperproduction of ROS by MDSC in cancer we used mice lacking gp91^{phox} and thus NOX2 activity (20). EL-4 tumor was established in wild-type (WT) and gp91^{phox}-deficient mice and the level of ROS was measured in MDSC 3 wk after tumor inoculation. *gp91$^{phox-/-}$* mice demonstrated slightly reduced tumor growth compared with WT mice, those differences were not statistically significant (data not shown). However, in contrast to their WT counterparts, gp91^{phox}-deficient MDSC from tumor-bearing mice showed no increase in the level of ROS when compared with MDSC from tumor-free mice (Fig. 4*A*). Previous studies have implicated ROS in Ag-specific T cell suppression (12) and in the inability of MDSC to differentiate into mature myeloid

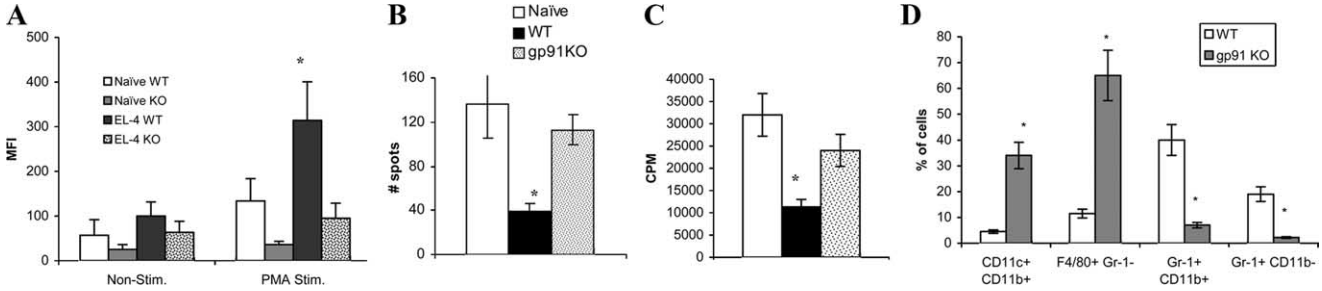

FIGURE 4. NOX2 is responsible for ROS production in MDSC and the Ag-specific immune suppression mediated by these cells. *A*, Production of ROS was evaluated in splenic Gr-1$^+$CD11b$^+$ MDSC from EL-4 tumor-bearing and gp91^{phox} knockout mice using staining with DCFDA. Each group included five mice. ∗, Statistically significant difference ($p < 0.05$) between WT and gp91$^{phox-/-}$ tumor-bearing mice. *B* and *C*, Gr-1$^+$ cells were isolated from naive, WT, or gp91^{phox} KO mice and were cultured with 1×10^5 splenocytes from OT-1 transgenic mice. IFN-γ production (*B*) and cell proliferation (*C*) were determined after stimulation with OVA-derived specific or control peptide (10 μg/ml) as described in *Materials and Methods*. The values obtained from cells stimulated with control peptides were subtracted from values from cells stimulated with specific peptide. Each experiment was performed in triplicates and repeated three times. Mean and SD for one representative experiment is shown. ∗, Statistically significant difference ($p < 0.05$) from naive MDSC. *D*, Gr-1$^+$CD11b$^+$ cells were isolated from WT and gp91 KO tumor-bearing mice and cultured with 20 ng/ml GM-CSF and 25% v/v TCCM for 5 days. Cell phenotype was evaluated by flow cytometry. Cumulative results from three performed experiments are shown. ∗, Statistically significant difference ($p < 0.05$) from WT MDSC.

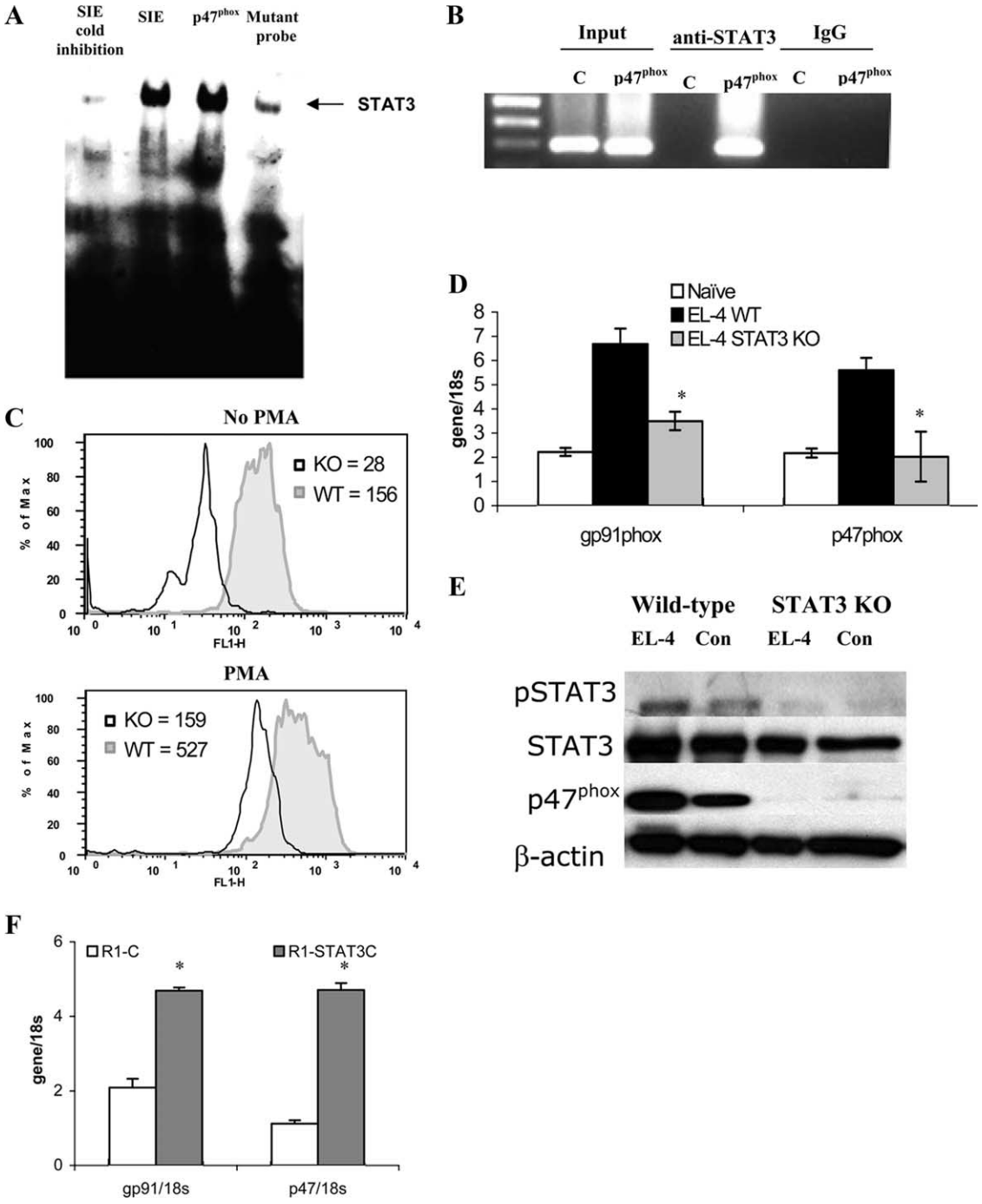

FIGURE 5. STAT3 regulates expression of NADPH oxidase. *A* and *B*, Nuclear extracts from STAT3C-transfected ES cells were prepared and used in EMSA. SIE: Conventional STAT3 specific probe, p47^{phox} sequence derived from promoter region of p47^{phox}. Mutant probe: Mutant p47^{phox}-derived probe. SIE cold inhibition: Binding to p47^{phox}-derived probe in the presence of 50-fold excess of unlabeled SIE probe. *B*, ChIP assay. DNA from 32D cells was precipitated with either anti-STAT3 Ab (STAT3) or control rabbit IgG (IgG). PCR was performed with primers specific for promoter regions of p47^{phox} or β-actin genes (*C*). Input: PCR performed with DNA isolated from nuclear extract without precipitation. *C–E*, EL-4 tumor cells were injected into wild-type (WT) or STAT3 knockout (KO) mice. Cells from the peritoneum were flushed out and collected 21 days after injection of EL-4 cells. To recruit macrophages, thioglycollate was injected i.p. 3 days before sacrificing animals. Peritoneal cells were stained with anti-CD11b Ab and production of ROS was analyzed (*C*). CD11b$^+$ macrophages were isolated from peritoneum of wild-type (WT) or STAT3$^{-/-}$ (KO) mice. The expression of p47^{phox} was assessed by real-time PCR (*D*) and amount of p47^{phox} protein was determined by Western blotting (*E*). *F*, R1-ES cells were transfected with either control plasmid (R1-C) or Stat3C plasmid (R1-Stat3C) (18). Expression of gp91^{phox} and p47^{phox} after transfection was determined.

cells (8). We asked whether lack of NOX2 activity affected those features of MDSC. Gr-1$^+$CD11b$^+$ cells were isolated from spleens of naive tumor-free mice, spleens of WT EL-4 tumor-bearing mice and *gp91$^{phox-/-}$* EL-4 tumor-bearing mice. Consistent with results reported earlier, MDSC from tumor-bearing mice induced significant suppression of IFN-γ production and proliferation of Ag-specific CD8$^+$ T cells in response to stimulation with a specific peptide (Fig. 4, *B* and *C*). In striking contrast, MDSC from NOX2-deficient mice failed to suppress T cell function (Fig. 4, *B* and *C*). To evaluate the effect of NOX2 on MDSC

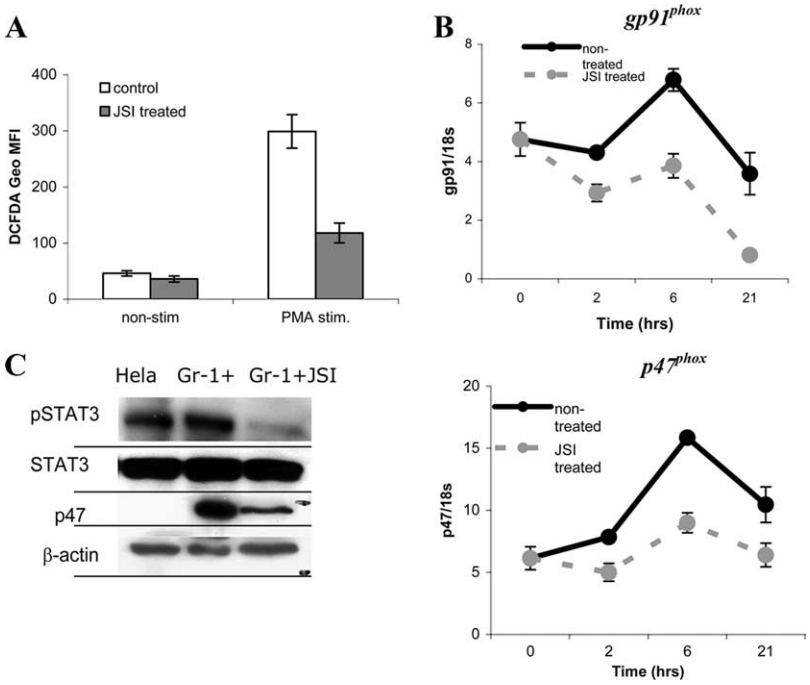

FIGURE 6. Effect of STAT3 inhibitor JSI-124 on ROS level in MDSC. Gr-1$^+$ cells were isolated from spleens of 3-wk MC38 tumor-bearing mice. Cells were cultured with tumor-cell-conditioned medium for 24 h and treated with the STAT3 inhibitor, JSI-124 (1.5 μM). *A*, ROS level measured in Gr-1$^+$CD11b$^+$ cells using DCFDA staining. *B*, Expression of *gp91^{phox}* and *p47^{phox}* at different time points after treatment with JSI-124 was evaluated using qRT-PCR. *C*, Levels of p47^{phox} protein in JSI-124 treated Gr-1$^+$CD11b$^+$ cells were analyzed by Western blotting. Hela cells were used as a positive control for phosphorylated STAT3.

differentiation, Gr-1$^+$CD11b$^+$ cells isolated from WT and *gp91$^{phox-/-}$* tumor-bearing mice were cultured in vitro for 5 days with GM-CSF in the presence of tumor-cell-conditioned medium (TCCM). Almost 40% of MDSC from WT mice retained the immature phenotype (Gr-1$^+$CD11b$^+$), with a small proportion of cells differentiating to either dendritic cells or macrophages. In contrast, the majority of MDSC from *gp91$^{phox-/-}$* tumor-bearing mice differentiated to F4/80$^+$Gr-1$^-$ macrophages or CD11c$^+$CD11b$^+$ dendritic cells (Fig. 4*D*). Thus, these data demonstrated that NOX2 was primarily responsible for the increased ROS level in spleen MDSC and for ROS-mediated functions of these cells.

Mechanisms regulating NOX2 in MDSC

We then went on to investigate how the level of NOX2 expression is regulated in splenic MDSC. We have previously shown that the STAT3 transcription factor plays a critical role in accumulation of MDSC in tumor-bearing mice (21, 22). We suggested that STAT3 could be involved in the increased NOX2 levels in MDSC. To our knowledge there was no information about the potential regulation of NOX2 by STAT3. To assess the role of STAT3 in regulation of NOX2, we selected one subunit-*p47^{phox}*. The promoter region of this gene contains the sequence TTCCCAGAG, which differs from the consensus STAT3 binding sequence TTCCCAGAA by one nucleotide. To verify that these two sequences had similar binding pattern, ES cells were transfected with a constitutively active STAT3 construct (21). Nuclear extract was prepared and binding of probes containing the consensus STAT3 binding sequence and p47^{phox} promoter-derived sequence was assessed by EMSA. Both probes showed the same pattern of binding. Importantly, binding of the *p47^{phox}*-derived probe was completely blocked by nonlabeled probe containing the STAT3 consensus sequence (Fig. 5*A*). To determine whether STAT3 could bind the *p47^{phox}* promoter, a ChIP assay was performed. As shown in Fig. 5*B*, anti-STAT3 Ab precipitated DNA that was amplified by primers specific for the *p47^{phox}* promoter region, indicating STAT3 binding to the *p47^{phox}* promoter.

To investigate the requirement of STAT3 for ROS production and *p47^{phox}* expression in MDSC, we used mice with a targeted disruption of STAT3 in myeloid cells (23). EL-4 tumors were established in STAT3 knockout (KO) mice or their WT littermates. Because lack of STAT3 prevented the development of MDSC (Ref. 22 and data not shown) we evaluated the effect of STAT3 disruption of NOX2 in CD11b$^+$ macrophages. Cells from the peritoneum were collected 3 days after injection of thioglycollate, labeled with anti-CD11b Ab, and their ability to generate ROS was analyzed. Both spontaneous and PMA-inducible levels of ROS in STAT3-deficient CD11b$^+$ cells were substantially lower than that in their WT counterparts (Fig. 5*C*). CD11b$^+$ macrophages were isolated from the peritoneum of tumor-free and tumor-bearing WT or STAT3$^{-/-}$ mice and the expression of *p47^{phox}* evaluated by qRT-PCR. Disruption of STAT3 resulted in significant reduction in the expression of *p47^{phox}* and *gp91^{phox}* genes (Fig. 5*D*) and protein (Fig. 5*E*). To assess the effect of over-expression of STAT3 on NOX2, ES cells were transfected with a constitutively active STAT3 mutant (STAT3C) (18). Normally, ES cells cultured in the presence of LIF display functionally active phospho-STAT3. LIF withdrawal leads to a substantial decrease in pY^{705}STAT3 within 48 h (24). Overexpression of STAT3C in ES cells prevented down-regulation of pY-STAT3 and resulted in a substantial increase in the expression of *gp91^{phox}* and *p47^{phox}* (Fig. 5*F*). Taken together, these data indicate that STAT3 directly regulates NOX2 expression and ROS production in myeloid cells.

The selective STAT3 inhibitor JSI-124 (25) has been previously shown to down-regulate STAT3 activity in MDSC and to dramatically reduce their presence in tumor-bearing mice (22). Treatment of tumor-bearing mice with JSI-124 substantially enhanced the effect of cancer immunotherapy and antitumor immune responses (22, 26, 27). We therefore asked whether JSI-124 mediates its effect via ROS down-regulation in MDSC. MDSC were isolated from spleens of 3-wk MC38 tumor-bearing mice and treated with JSI-124 in the presence of TCCM. Twenty-four hour treatment with the STAT3 inhibitor dramatically ($p < 0.01$) reduced the level of ROS in these cells (Fig. 6*A*). JSI-124 caused a decrease in the expression of *p47^{phox}* and *gp91^{phox}* as early as 6 h after the start of treatment (Fig. 6*B*). JSI-124 treatment also resulted in a substantial decrease in the level of p47^{phox} protein in these cells (Fig. 6*C*).

Discussion

Recent years have provided ample evidence supporting the important role of ROS in MDSC-mediated suppression of T cells (10, 14, 15, 28–31). However, those study were performed on a very limited number of models and, most importantly, these studies did not clarify the reason for the increase in ROS levels in these cells. In this study, we have demonstrated that up-regulation of ROS in MDSC is a common phenomenon observed in a variety of different tumor models. Importantly, this phenomenon was observed in human MDSC as well. This by itself is not very surprising but reinforces the potentially important role of ROS up-regulation in MDSC-mediated effects in cancer. Although cells can use multiple mechanisms for ROS generation, in leukocytes the primary producer of ROS is NADPH oxidase. NADPH oxidase catalyzes the one-electron reduction of oxygen to superoxide anion using electrons supplied by NADPH. The importance of this enzyme can be observed in the severity of hereditary chronic granulomatous disease (CGD). CGD is caused by mutations in any of the genes that encode the subunits of the oxidase and patients with CGD experience frequent life-threatening infections during their lifetime (32). The oxidase is a multicomponent enzyme consisting of two membrane proteins, gp91 and p22, that together form a unique membrane-bound flavocytochrome and at least four cytosolic components: $p47^{phox}$, $p67^{phox}$, $p40^{phox}$, and a small G protein Rac (19). In leukocytes, increased ROS production in response to different stimuli is regulated primarily by activation of NOX2 via assembly of the enzymatic complex on the cellular membrane after translocation from the cytoplasm. The response usually does not involve transcriptional regulation of subunits of the NADPH complex. However, our data demonstrate that in MDSC from tumor-bearing mice, up-regulation of NOX2 activity and ROS production involves substantial increase in the expression of several NOX2 subunits. In this situation even slight stimulation of these cells that would normally induce minimal NOX2 activation would result in a substantial production of ROS. An example of such stimuli could be an interaction of MDSC with activated T cells, endothelial cells, or fibroblasts in tissues. Under normal conditions, in the absence of injury, contact of myeloid cells with surrounding cells would result in very modest up-regulation of ROS, which is primarily mediated by adhesion molecules (33). However, in the condition of constitutive up-regulation of NOX2 expression in MDSC, the same interaction results in dramatic increase in ROS production in these cells. This may explain the previously reported fact that direct cell-cell contact with Ag-specific $CD8^+$ T cells caused substantially higher level of ROS in MDSC then in IMC (12). This effect was shown to be mediated by integrins.

MDSC with deleted $gp91^{phox}$ gene, thus lacking NOX2 activity, did not demonstrate increased ROS level compared with IMC from naive mice. Notably, lack of NOX2 activity also abrogated major functions of MDSC attributed to ROS. This strongly suggest that up-regulation of ROS in these cells in cancer is controlled by NOX2 activity. Lack of NOX2 did not result in tumor rejection in these mice underscoring the fact that tumor escape mechanisms could not be ascribed to only one factor.

What could be the mechanism of NOX2 up-regulation in MDSC? MDSC expansion in tumor-bearing hosts is mediated by various tumor-derived factors (1). STAT3 is arguably one of the main transcription factors responsible for MDSC accumulation in cancer. Signaling from many tumor-derived factors implicated in MDSC expansion ultimately converge in the Jak/STAT3 pathway (34, 35). Consequently, MDSCs from tumor bearing mice have dramatically increased levels of phosphorylated STAT3 compared with IMC from naive mice (22). Exposure of hematopoietic progenitor cells to tumor-cell-conditioned medium resulted in the activation of STAT3 and was associated with an expansion of MDSCs in vitro, whereas inhibition of STAT3 in these cells abrogated the effect of tumor-derived factors on MDSC expansion (21). Ablation of STAT3 using conditional-KO mice or selective inhibitors dramatically reduced the expansion of MDSCs and improved T cell responses in tumor-bearing mice (22, 36). Thus, it appears that abnormal persistent activation of STAT3 in myeloid progenitors prevents differentiation of myeloid cells and is associated with increased proliferation and survival of myeloid progenitors, possibly through up-regulation of STAT3-targeted genes like Bcl-xL, cyclin D1, c-*myc*, survivin (35), or S100A8 and S100A9 proteins (24). Our data for the first time have demonstrated that STAT3 directly regulates expression of $p47^{phox}$, the main component of the NOX2 complex and possibly $gp91^{phox}$, the other critical subunit of NOX2. These results provide a direct link between various tumor-derived factors affecting MDSC and the level of ROS in these cells. The critical role of STAT3 in regulation of ROS in MDSC was further confirmed in experiments with JSI-124, a selective STAT3 inhibitor (25). We have previously demonstrated that JSI-124 has potent effect on MDSC in vitro and in vivo (22, 37). This study provides mechanism of the effect of JSI-124 downstream of STAT3.

Thus, this study suggests a novel mechanism that regulates ROS in MDSC during cancer. Tumor-derived factors, via constitutive up-regulation of STAT3 transcription factors, induced expansion of MDSC that contain high level of components of NADPH oxidase. This makes MDSC in tumor-bearing mice prone to respond to different stimuli including contact with surrounding cells with increased ROS production, which would contribute to immune suppressive activity of these cells. This suggests that NOX2 could be an attractive target in therapeutic regulation of MDSC function.

Acknowledgments

We thank Dr. Edward Visse (University of Lund, Sweden) for help at the beginning of this project.

Disclosures

The authors have no financial conflict of interest.

References

1. Kusmartsev, S., and D. I. Gabrilovich. 2006. Role of immature myeloid cells in mechanisms of immune evasion in cancer. *Cancer Immunol Immunother.* 55: 237–245.
2. Sica, A., and V. Bronte. 2007. Altered macrophage differentiation and immune dysfunction in tumor development. *J. Clin. Invest.* 117: 1155–1166.
3. Talmadge, J. E. 2007. Pathways mediating the expansion and immunosuppressive activity of myeloid-derived suppressor cells and their relevance to cancer therapy. *Clin Cancer Res.* 13: 5243–5248.
4. Rabinovich, G. A., D. Gabrilovich, and E. M. Sotomayor. 2007. Immunosuppressive strategies that are mediated by tumor cells. *Annu. Rev. Immunol.* 25: 267–296.
5. Almand, B., J. I. Clark, E. Nikitina, N. R. English, S. C. Knight, D. P. Carbone, and D. I. Gabrilovich. 2001. Increased production of immature myeloid cells in cancer patients: a mechanism of immunosuppression in cancer. *J. Immunol.* 166: 678–689.
6. Zea, A. H., P. C. Rodriguez, M. B. Atkins, C. Hernandez, S. Signoretti, J. Zabaleta, D. McDermott, D. Quiceno, A. Youmans, A. O'Neill, et al. 2005. Arginase-producing myeloid suppressor cells in renal cell carcinoma patients: a mechanism of tumor evasion. *Cancer Res.* 65: 3044–3048.
7. Diaz-Montero, C. M., M. L. Salem, M. I. Nishimura, E. Garrett-Mayer, D. J. Cole, and A. J. Montero. 2009. Increased circulating myeloid-derived suppressor cells correlate with clinical cancer stage, metastatic tumor burden, and doxorubicin-cyclophosphamide chemotherapy. *Cancer Immunol. Immunother.* 58: 49–59.
8. Kusmartsev, S., and D. I. Gabrilovich. 2003. Inhibition of myeloid cell differentiation in cancer: the role of reactive oxygen species. *J. Leukocyte Biol.* 74: 186–196.
9. Movahedi, K., M. Guilliams, J. Van den Bossche, R. Van den Bergh, C. Gysemans, A. Beschin, P. De Baetselier, and J. A. Van Ginderachter. 2008. Identification of discrete tumor-induced myeloid-derived suppressor cell subpopulations with distinct T-cell suppressive activity. *Blood* 111: 4233–4244.

10. Nagaraj, S., K. Gupta, V. Pisarev, L. Kinarsky, S. Sherman, L. Kang, D. Herber, J. Schneck, and D. Gabrilovich. 2007. Altered recognition of antigen is a novel mechanism of $CD8^+$ T cell tolerance in cancer. *Nat. Med.* 13: 828–835.
11. Kusmartsev, S., S. Nagaraj, and D. I. Gabrilovich. 2005. Tumor-associated $CD8^+$ T cell tolerance induced by bone marrow-derived immature myeloid cells. *J. Immunol.* 175: 4583–4592.
12. Kusmartsev, S., Y. Nefedova, D. Yoder, and D. I. Gabrilovich. 2004. Antigen-specific inhibition of $CD8^+$ T cell response by immature myeloid cells in cancer is mediated by reactive oxygen species. *J. Immunol.* 172: 989–999.
13. Sinha, P., V. K. Clements, and S. Ostrand-Rosenberg. 2005. Reduction of myeloid-derived suppressor cells and induction of M1 macrophages facilitate the rejection of established metastatic disease. *J. Immunol.* 174: 636–645.
14. Nefedova, Y., M. Fishman, S. Sherman, X. Wang, A. A. Beg, and D. I. Gabrilovich. 2007. Mechanism of all-trans retinoic acid effect on tumor-associated myeloid-derived suppressor cells. *Cancer Res.* 67: 11021–11028.
15. Markiewski, M. M., R. A. DeAngelis, F. Benencia, S. K. Ricklin-Lichtsteiner, A. Koutoulaki, C. Gerard, G. Coukos, and J. D. Lambris. 2008. Modulation of the antitumor immune response by complement. *Nat Immunol.* 9: 1225–1235.
16. Ando, T., K. Mimura, C. C. Johansson, M. G. Hanson, D. Mougiakakos, C. Larsson, T. Martins da Palma, D. Sakurai, H. Norell, M. Li, et al. 2008. Transduction with the antioxidant enzyme catalase protects human T cells against oxidative stress. *J. Immunol.* 181: 8382–8390.
17. Mirza, N., M. Fishman, I. Fricke, M. Dunn, A. Neuger, T. Frost, R. Lush, S. Antonia, and D. Gabrilovich. 2006. All-trans-retinoic acid improves differentiation of myeloid cells and immune response in cancer patients. *Cancer Res.* 66: 9299–9307.
18. Bromberg, J. F., M. H. Wrzeszczynska, G. Devgan, Y. Zhao, R. G. Pestell, C. Albanese, and J. E. Darnell. 1999. Stat3 as an oncogene. *Cell* 98: 295–303.
19. Groemping, Y., and K. Rittinger. 2005. Activation and assembly of the NADPH oxidase: a structural perspective. *Biochem. J.* 386: 401–416.
20. Quinn, M. T. 2005. The neutrophils respiratory burst oxidase. In *The Neutrophils: New Outlook for Old Cells.*, 2nd ed. D. I. Gabrilovich, ed. Imperial College Press, London, pp. 35–85.
21. Nefedova, Y., M. Huang, S. Kusmartsev, R. Bhattacharya, P. Cheng, R. Salup, R. Jove, and D. Gabrilovich. 2004. Hyperactivation of STAT3 is involved in abnormal differentiation of dendritic cells in cancer. *J. Immunol.* 172: 464–474.
22. Nefedova, Y., S. Nagaraj, A. Rosenbauer, C. Muro-Cacho, S. M. Sebti, and D. I. Gabrilovich. 2005. Regulation of dendritic cell differentiation and antitumor immune response in cancer by pharmacologic-selective inhibition of the Janus-activated kinase 2/signal transducers and activators of transcription 3 pathway. *Cancer Res.* 65: 9525–9535.
23. Takeda, K., B. E. Clausen, T. Kaisho, T. Tsujimura, N. Terada, I. Forster, and S. Akira. 1999. Enhanced Th1 activity and development of chronic enterocolitis in mice devoid of Stat3 in macrophages and neutrophils. *Immunity* 10: 39–49.
24. Cheng, P., C. A. Corzo, N. Luetteke, B. Yu, S. Nagaraj, M. M. Bui, M. Ortiz, W. Nacken, C. Sorg, T. Vogl, et al. 2008. Inhibition of dendritic cell differentiation and accumulation of myeloid-derived suppressor cells in cancer is regulated by S100A9 protein. *J. Exp. Med.* 205: 3325–2249.
25. Blaskovich, M. A., J. Sun, A. Cantor, J. Turkson, R. Jove, and S. M. Sebti. 2003. Discovery of JSI-124 (Cucurbitacin I), a selective Janus kinase/signal transducer and activator of transcription 3 signaling pathway inhibitor with potent antitumor activity against human and murine cancer cells in mice. *Cancer Res.* 63: 1270–1279.
26. Fujita, M., X. Zhu, K. Sasaki, R. Ueda, K. L. Low, I. F. Pollack, and H. Okada. 2008. Inhibition of STAT3 promotes the efficacy of adoptive transfer therapy using type-1 CTLs by modulation of the immunological microenvironment in a murine intracranial glioma. *J. Immunol.* 180: 2089–2098.
27. Molavi, O., Z. Ma, S. Hamdy, R. Lai, A. Lavasanifar, and J. Samuel. 2008 Synergistic antitumor effects of CpG oligodeoxynucleotide and STAT3 inhibitory agent JSI-124 in a mouse melanoma tumor model. *Immunol. Cell Biol.* 86: 506–514.
28. Kusmartsev, S., Z. Su, A. Heiser, J. Dannull, E. Eruslanov, H. Kubler, D. Yancey, P. Dahm, and J. Vieweg. 2008. Reversal of myeloid cell-mediated immunosuppression in patients with metastatic renal cell carcinoma. *Clin. Cancer Res.* 14: 8270–8278.
29. Youn, J. I., S. Nagaraj, M. Collazo, and D. I. Gabrilovich. 2008. Subsets of myeloid-derived suppressor cells in tumor-bearing mice. *J. Immunol.* 181: 5791–5802.
30. Mougiakakos, D., C. C. Johansson, and R. Kiessling. 2008. Naturally occurring regulatory T cells show reduced sensitivity towards oxidative stress induced cell death. *Blood In press*.
31. Sinha, P., V. Clements, and S. Ostrand-Rosenberg. 2005. Reduction of myeloid-derived suppressor cells and induction of M1 macrophages facilitate the rejection of established metastatic disease. *J. Immunol.* 174: 636–645.
32. Assari, T. 2006. Chronic granulomatous disease; fundamental stages in our understanding of CGD. *Med Immunol.* 5: 4.
33. Forman, H. J., and M. Torres. 2001. Redox signaling in macrophages. *Mol. Aspects Med.* 22: 189–216.
34. Gabrilovich, D. I. 2004. The mechanisms and functional significance of tumour-induced dendritic-cell defects. *Nat. Rev. Immunol.* 4: 941–952.
35. Nefedova, Y., and D. I. Gabrilovich. 2007. Targeting of Jak/STAT pathway in antigen presenting cells in cancer. *Curr. Cancer Drug Targets* 7: 71–77.
36. Kortylewski, M., M. Kujawski, T. Wang, S. Wei, S. Zhang, S. Pilon-Thomas, G. Niu, H. Kay, J. Mule, W. G. Kerr, et al. 2005. Inhibiting Stat3 signaling in the hematopoietic system elicits multicomponent antitumor immunity. *Nat. Med.* 11: 1314–1321.
37. Nefedova, Y., P. Cheng, D. Gilkes, M. Blaskovich, A. A. Beg, S. M. Sebti, and D. I. Gabrilovich. 2005. Activation of dendritic cells via inhibition of Jak2/STAT3 signaling. *J. Immunol.* 175: 4338–4346.